ELSEVIER

www.elsevier.nl/locate/jorganchem

Journal of Organometallic Chemistry 616 (2000) 140–148

Journal of Organo metallic Chemistry

Syntheses, spectroscopic characterization and electrochemical properties of organometallic crown ethers containing tetrahedral $W_2Fe(\mu_3\text{-}S)$ cluster cores $[W_2Fe(\mu_3\text{-}S)(CO)_7][\eta^5\text{-}C_5H_4CH_2\text{-}(CH_2OCH_2)_nCH_2C_5H_4\text{-}\eta^5]$ ($n = 1$–3). Crystal structures of $[W_2Fe(\mu_3\text{-}S)(CO)_7][\eta^5\text{-}C_5H_4CH_2(CH_2OCH_2)_nCH_2C_5H_4\text{-}\eta^5]$ ($n = 2,3$)

Li-Cheng Song [a,*], Dian-Shun Guo [a], Qing-Mei Hu [a], Jie Sun [b]

[a] *Department of Chemistry, State Key Laboratory of Elemento-Organic Chemistry, Nankai University, Tianjin 300071, People's Republic of China*

[b] *Laboratory of Organometallic Chemistry, Chinese Academy of Sciences, Shanghai 200032, People's Republic of China*

Received 9 June 2000; received in revised form 16 August 2000; accepted 23 August 2000

Abstract

The self-assembly cyclization reactions of the ether chain-bridged dicyclopentadienyl W/Na salts $Na_2[\{W(CO)_3\}_2\{\eta^5\text{-}C_5H_4CH_2(CH_2OCH_2)_nCH_2C_5H_4\text{-}\eta^5\}]$ (**Ia**–**c**, $n = 1$–3) with the same chain-bridged dicyclopentadienyl double clusters $[WCoFe(\mu_3\text{-}S)(CO)_8]_2[\eta^5\text{-}C_5H_4CH_2(CH_2OCH_2)_nCH_2C_5H_4\text{-}\eta^5]$ (**IIa**–**c**, $n = 1$–3) have been shown to give organometallic crown ethers $[W_2Fe(\mu_3\text{-}S)(CO)_7][\eta^5\text{-}C_5H_4CH_2\ (CH_2OCH_2)_nCH_2C_5H_4\text{-}\eta^5]$ (**IIIa**–**c**, $n = 1$–3). While structures of these new $W_2Fe(\mu_3\text{-}S)$ cluster crown ethers were fully characterized by elemental analyses, IR, ^{1}H-NMR and FAB-MS spectroscopies, those of **IIIb**,**c** were unambiguously confirmed by X-ray diffraction techniques. In the study of possible pathway for the formation of **IIIa**–**c**, the new cluster crown ether **IIIc** and its known Mo analog $[Mo_2Fe(\mu_3\text{-}S)(CO)_7][\eta^5\text{-}C_5H_4CH_2(CH_2OCH_2)_3CH_2C_5H_4\text{-}\eta^5]$ (**IV**) were also found to be formed through self-assembly cyclization reaction of the W/Na salt $Na_2[\{W(CO)_3\}_2\{\eta^5\text{-}C_5H_4CH_2(CH_2OCH_2)_3\text{-}CH_2C_5H_4\text{-}\eta^5\}]$ and the corresponding Mo-containing double cluster $[MoCoFe(\mu_3\text{-}S)(CO)_8]_2[\eta^5\text{-}C_5H_4CH_2(CH_2OCH_2)_3CH_2C_5H_4\text{-}\eta^5]$. In addition, the electrochemical properties of **IIIa**–**c** have been studied by cyclic voltammetric techniques. © 2000 Elsevier Science B.V. All rights reserved.

Keywords: Tungsten; Iron; Cobalt; Crown ether; Crystal structures

---

1. Introduction

Recently, the crown ethers have received increasing attention, largely due to their unique properties and important applications in areas such as catalysis, molecular and ion recognition, and sensor technology, etc. [1–5]. Among crown ethers, the organometallic ones that contain both crown ether and organometallic structural units are of particular interest, since the affinity of the crown ether subunit toward metal complexation can be regulated by the oxidation state of the redox-active metal centers in their organometallic subunits. So far, although a variety of organometallic crown ethers are known [6–17], only a few of them possess transition metal cluster cores, which contain tetrahedral $Mo_2Fe(\mu_3\text{-}S)$ cluster cores and have been prepared from a novel type of self-assembly cyclization reaction [6]. In order to synthesize their tungsten analogs and examine the scope of application of this novel cyclization reaction, we initiated this study. Herein we report the results by describing the synthetic method, spectroscopic characterization and electrochemical properties of three tetrahedral $W_2Fe(\mu_3\text{-}S)$ cluster crown ethers $[W_2Fe(\mu_3\text{-}S)(CO)_7][\eta^5\text{-}C_5H_4CH_2\text{-}(CH_2OCH_2)_nCH_2C_5H_4\text{-}\eta^5]$ (**IIIa**, $n = 1$; **IIIb**, $n = 2$; **IIIc**, $n = 3$), as well as the crystal structures of **IIIb**,**c** determined by X-ray diffraction techniques.

---

* Corresponding author. Fax: +86-22-23504853.

E-mail address: lcsong@public.tpt.tj.cn (L.-C. Song).

PII: S0022-328X(00)00584-2

2. Results and discussion

2.1. Synthesis and spectroscopic characterization of $[W_2Fe(\mu_3\text{-}S)(CO)_7][\eta^5\text{-}C_5H_4CH_2(CH_2OCH_2)_n\text{-}CH_2C_5H_4\text{-}\eta^5]$ (**IIIa–c**, $n = 1–3$)

We found that the ether chain-bridged dicyclopentadienyl W/Na salts $Na_2[\{W(CO)_3\}_2\{\eta^5\text{-}C_5H_4CH_2(CH_2OCH_2)_nCH_2C_5H_4\text{-}\eta^5\}]$ (**Ia**–**c**, $n = 1–3$) reacted with the same chain-bridged dicyclopentadienyl double clusters $[WCoFe(\mu_3\text{-}S)(CO)_8]_2[\eta^5\text{-}C_5H_4CH_2(CH_2OCH_2)_nCH_2\text{-}C_5H_4\text{-}\eta^5]$ (**IIa**–**c**, $n = 1–3$) in THF at reflux to give three tetrahedral $W_2Fe(\mu_3\text{-}S)$ cluster crown ethers $[W_2Fe(\mu_3\text{-}S)(CO)_7][\eta^5\text{-}C_5H_4CH_2(CH_2OCH_2)_nCH_2C_5\text{-}H_4\text{-}\eta^5]$ (**IIIa**–**c**, $n = 1–3$), as shown in Scheme 1.

It should be pointed out that the W/Na salts **Ia**–**c** used in the preparation of **IIIa**–**c** were prepared from disodium salts $Na_2[\eta^5\text{-}C_5H_4CH_2(CH_2OCH_2)_nCH_2C_5H_4\text{-}\eta^5]$ ($n = 1–3$) with $W(CO)_6$ in diglyme [18,19], and the yields of **IIIa**–**c** obtained from this reaction sequence are 8, 20 and 29% (calculated based on **IIa**–**c**), respectively.

Products **IIIa**–**c** are air stable and black solids, which have been characterized by elemental analysis, IR, ^{1}H-NMR and FAB-MS spectroscopies. The IR spectra of **IIIa**–**c** display 5–7 absorption bands in the range 2026–1815 cm^{-1} for their terminal [20] and semibridging [21] carbonyls, as well as one absorption band in the range 1127–1108 cm^{-1} for their bridged ether chain functionalities [22]. In the ^{1}H-NMR spectra of **IIIa**–**c** there are two multiplets in the ranges 2.63–3.19 and 3.47–3.82 ppm for α-CH_2 attached to Cp rings and their neighboring β-CH_2 (for **IIIb**,**c** the latter range also contains the other CH_2 signals), respectively. Furthermore, in their ^{1}H-NMR spectra there are two sets of two singlets in the range 5.03–5.69 ppm for the substituted Cp protons, the upfield set being assigned to H^2/H^5 close to the ether chain substituent and the downfield set to H^3/H^4 remote from the substituent [23]. It follows that the IR and ^{1}H-NMR behavior of **IIIa**–**c** is very similar to that of the Mo-containing analogs $[Mo_2Fe(\mu_3\text{-}S)(CO)_7][\eta^5\text{-}C_5H_4CH_2(CH_2OCH_2)_n\text{-}CH_2C_5H_4\text{-}\eta^5]$ [6]. The FAB-MS data of **IIIa**–**c** show their respective molecular ion M^+ and corresponding fragment ions by successive loss of a given number of CO and H atoms.

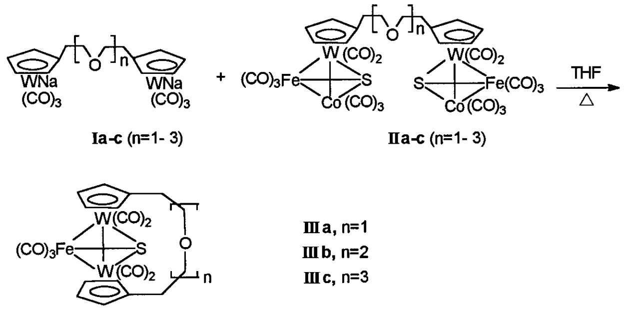

Scheme 1.

2.2. Crystal structures of $[W_2Fe(\mu_3\text{-}S)(CO)_7]\text{-}[\eta^5\text{-}C_5H_4CH_2(CH_2OCH_2)_2CH_2C_5H_4\text{-}\eta^5]$ (**IIIb**) and $[W_2Fe(\mu_3\text{-}S)(CO)_7][\eta^5\text{-}C_5H_4CH_2(CH_2OCH_2)_3\text{-}CH_2C_5H_4\text{-}\eta^5]$ (**IIIc**)

In order to confirm the structures of cluster crown ethers **IIIa**–**c**, the X-ray diffraction analyses for **IIIb**,**c** were undertaken. It is worth noting that although **IIIc** has two crystallographically independent molecules A and B in the unit cell, only A is discussed here, since A and B have almost identical structural parameters. Figs. 1 and 2 illustrate the molecular structures of **IIIb** and **IIIc**, respectively.

As seen from Figs. 1 and 2, both molecules are composed of a distorted tetrahedral $W_2Fe(\mu_3\text{-}S)$ cluster core, carrying one ether chain-bridged dicyclopentadienyl ligand coordinated to two W atoms, one set of three CO ligands attached to the Fe atom and two sets of two CO ligands attached to two W atoms, respectively. Apparently, they belong to the same type of macrocyclic cluster crown ethers with different lengths of bridging ether chains. For one of the cluster crown ethers with a given length of the bridging ether chain, for example **IIIc**, it can be viewed as a ring size-varied crown ether, depending on which carbon atoms of the two Cp rings, C8 through C12 and C21 through C25, and which atoms of the cluster core are involved in counting the cyclic size.

Tables 1 and 2 list the selected bond lengths and angles of **IIIb**,**c**, whereas Table 3 gives some of the dihedral angles. As seen from Tables 1–3, the bond lengths, bond angles, and dihedral angles of **IIIb** are very similar to the corresponding values of **IIIc**. However, for **IIIb**,**c** the dihedral angles between two planes of W_1FeW_2 and Cp(1) are remarkably different from those between W_1FeW_2 and Cp(2), which implies that the two molecules are asymmetric. So, the two α-hydrogen atoms attached to C13 or C18 (**IIIb**) and C13 or C20 (**IIIc**), and those β-hydrogen atoms attached to C14 or C17 (**IIIb**) and C14 or C19 (**IIIc**) are magnetically unequivalent and thus give the complicated ^{1}H-NMR spectral patterns as described above. Finally, the structural analysis of **IIIb** or **IIIc** shows that among its seven carbonyls there are three semibridging carbonyls and four terminal carbonyls. While the semibriging carbonyls of **IIIb** are C1O1, C3O3 and C4O4, those of **IIIc** are C2O2, C3O3 and C4O4. The asymmetric parameters α for these semibridging carbonyls [21] are given in Table 4, along with some of their important parameters.

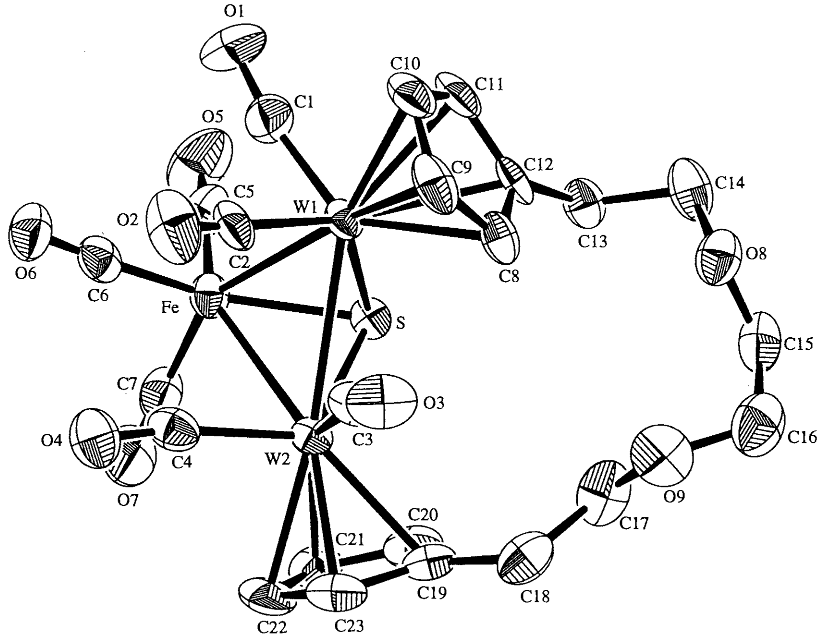

Fig. 1. ORTEP plot of **IIIb** with the atom labeling scheme.

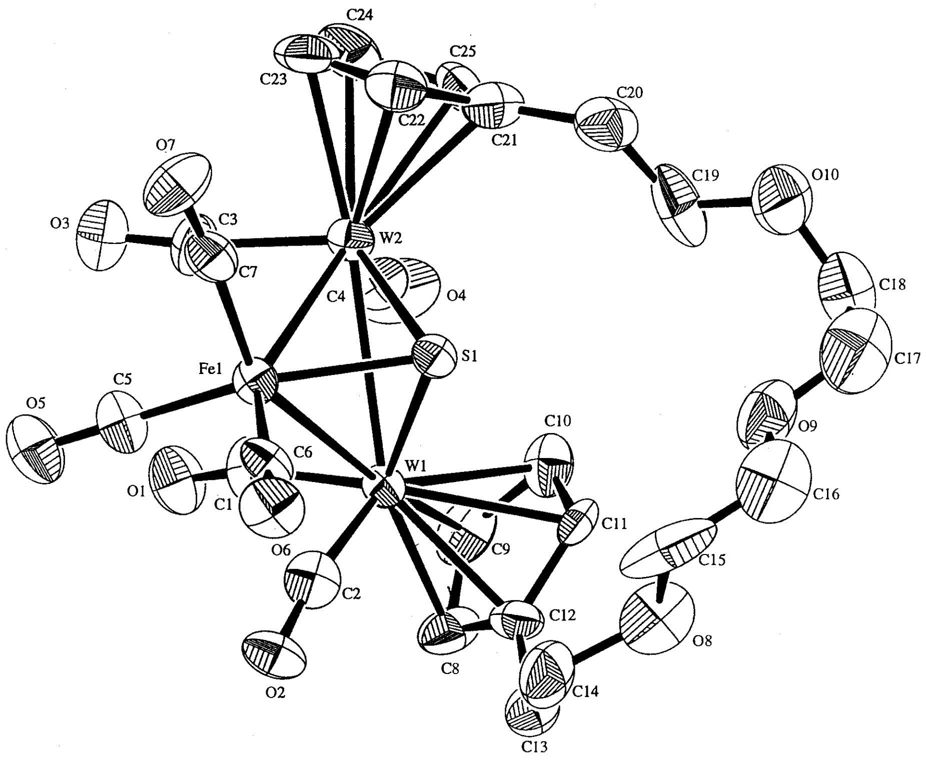

Fig. 2. ORTEP plot of **IIIc** with the atom labeling scheme.

So, the existence of both terminal and semibridging carbonyls confirmed by X-ray diffraction analyses coincides very well with the IR spectra of **IIIb**,**c** showing several absorption bands in the range 2026–1815 cm^{-1}.

2.3. *Possible pathway for the formation of* ***IIIa–c***

The possible pathway for the formation of **IIIa**–**c** is similar to that for the formation of their Mo analogs

Table 1
Selected bond lengths (Å) and angles (°) for **IIIb**

W1–W2	3.0385(5)	W–S	2.370(2)
W2–Fe	2.800(1)	W1–Fe	2.813(1)
W2–S	2.374(2)	Fe–S	2.206(2)
W1–C1	1.959(9)	Fe–C5	1.776(8)
W2–C3	1.930(7)	C12–C13	1.482(9)
C14–O8	1.395(9)	C16–O9	1.43(1)
W2–W1–Fe	57.01(2)	W2–W1–S	50.22(4)
Fe–W1–S	49.47(5)	W1–W2–S	50.12(4)
W1–W2–Fe	57.45(2)	Fe–W2–S	49.65(5)
W1–Fe–W2	65.55(2)	W1–Fe–S	54.75(5)
W2–Fe–S	55.08(5)	W1–S–Fe	75.78(6)

Table 2
Selected bond lengths (Å) and angles (°) for **IIIc**

W1–W2	3.030(1)	W1–Fe1	2.820(2)
W1–S1	2.409(4)	W2–S1	2.328(4)
W2–Fe1	2.753(3)	Fe1–S1	2.221(5)
W1–C1	1.97(2)	C12–C13	1.48(3)
W2–C3	1.94(2)	C14–O8	1.51(4)
Fe1–C5	1.77(2)	C16–O9	1.41(4)
W2–W1–Fe1	56.00(6)	W2–W1–S1	49.1(1)
Fe1–W1–S1	49.5(1)	W1–W2–S1	51.41(9)
W1–W2–Fe1	58.14(5)	Fe1–W2–S1	51.0(1)
W1–Fe1–W2	65.86(5)	W1–Fe1–S1	55.56(10)
W2–Fe1–S1	54.5(1)	W1–S1–Fe1	74.9(1)

Table 3
Some dihedral angles (°) for **IIIb**,**c**

IIIb [a]		IIIc [b]	
W1FeW2/Cp(1)	105.18	W1Fe1W2/Cp(1)	104.93
W1FeW2/Cp(2)	71.37	W1Fe1W2/Cp(2)	70.18
Cp(1)/Cp(2)	72.21	Cp(1)/Cp(2)	72.20

[a] Cp(1) = C8–C12, Cp(2) = C19–C23.
[b] Cp(1) = C8–C12, Cp(2) = C21–C25.

recently suggested [6] based on isolobal displacement modes [24–26] (Scheme 2).

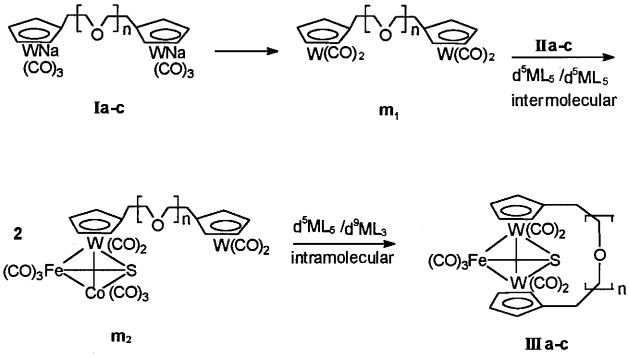

Scheme 2.

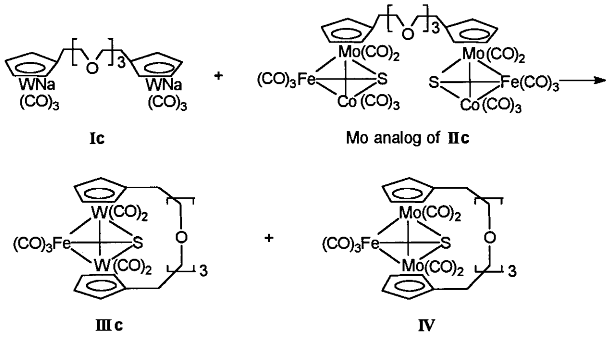

Scheme 3.

As shown in Scheme 2, the bridged W/Na salts **Ia**–**c** can be decarbonylated to give intermediates $\mathbf{m_1}$ and then they react with the bridged double clusters **IIa**–**c** through intermolecular single isolobal d^5ML_5/d^5ML_5 displacement to produce two molecules of intermediates $\mathbf{m_2}$. Finally, **IIIa**–**c** will be yielded from $\mathbf{m_2}$ by intramolecular single isolobal d^5ML_5/d^9ML_3 displacement.

In principle, the intermediates $\mathbf{m_2}$ could also be produced through a ligand exchange process between $\mathbf{m_1}$ and **IIa**–**c**. In order to exclude this possibility, we carried out a reaction of **Ic** with the Mo analog of **IIc**. Since from this reaction two crown ethers **IIIc** and its Mo analog [$Mo_2Fe(\mu_3$-S)(CO)$_7$][η^5-$C_5H_4CH_2(CH_2$-

Table 4
Semibridging COs for **IIIb**,**c** [a]

	d_1 (Å)		d_2 (Å)		α	θ (°)	
IIIb							
C1O1	W1–C1	1.959	Fe···C1	2.715	0.38	WC1O1	168.6
C3O3	W2–C3	1.930	W1···C3	2.896	0.50	W2C3O3	168.1
C4O4	W2–C4	1.977	Fe···C4	2.846	0.44	W2C4O4	170.5
IIIc							
C2O2	W1–C2	1.850	Fe1···C2	2.641	0.43	WC2O2	169.0
C3O3	W2–C4	1.990	W1···C4	2.999	0.50	W2C4O4	169.0
C4O4	W2–C3	1.940	Fe1···C3	2.863	0.47	W2C3O3	170.0

[a] The asymmetric parameter α is defined as $\alpha = d_2 - d_1/d_1$, where d_1 and d_2 are the short and long distances of M–C(O), respectively. If $0.1 \leq \alpha \leq 0.6$, a semibridging carbonyl is designated.

$OCH_2)_3CH_2C_5H_4$-η^5] (**IV**) [6] were obtained (Scheme 3), we might conclude that the intermediates $\mathbf{m_2}$ were generated most likely by isolobal displacement, not by ligand exchange. This is because that the ligand exchange between intermediates $\mathbf{m_1}$ and the Mo analogs **IIa–c** involves bond-breaking processes between the Cp ring and Mo or W atom to give only one type of intermediate that is subsequently converted to one type of corresponding product with a MoWFe(μ_3-S) cluster core, whereas the isolobal displacement in the same reaction does not involve such bond-breaking processes and thus affords two types of intermediates and finally two types of corresponding products, one with a $Mo_2Fe(\mu_3\text{-}S)$ cluster core and the other with a $W_2Fe(\mu_3\text{-}S)$ cluster core, as shown in Scheme 4.

Finally, it should be noted that according to the suggested pathway described in Scheme 2, the reaction of **Ia–c** with **IIa–c** could also produce other types of products. For example, if one molecule of the intermediates $\mathbf{m_1}$ reacts with **IIa–c** via intermolecular d^5ML_5/d^9ML_3 isolobal displacement or if two molecules of the intermediates $\mathbf{m_2}$ undergo intermolecular d^5ML_5/d^9ML_3 isolobal displacement, the intermediates $\mathbf{m_3}$ will be formed; Then, if this type of intermediate undergoes intramolecular d^5ML_5/d^9ML_3 isolobal displacement, the cyclic dimers of type **V** will be produced (Scheme 5). In fact, type **V** with $n = 3$ was separated by TLC, but it was only recognized by IR and ^{1}H-NMR spectroscopy because it was produced in too small an amount. In addition, such a type of cyclic dimer for the Mo-containing analog was separated in 17% yield from the corresponding reaction and this dimer has been fully characterized by elemental analysis and spectroscopic techniques.

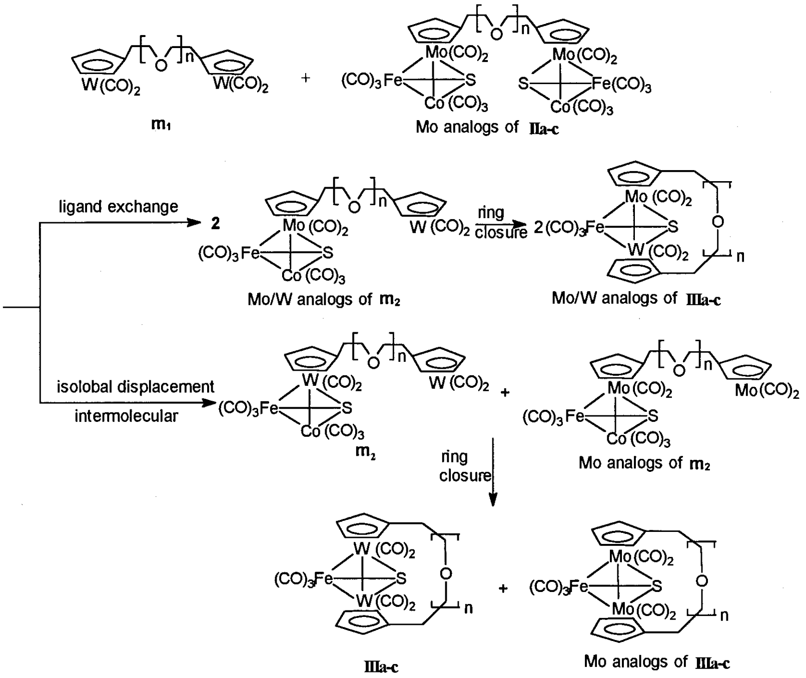

Scheme 4.

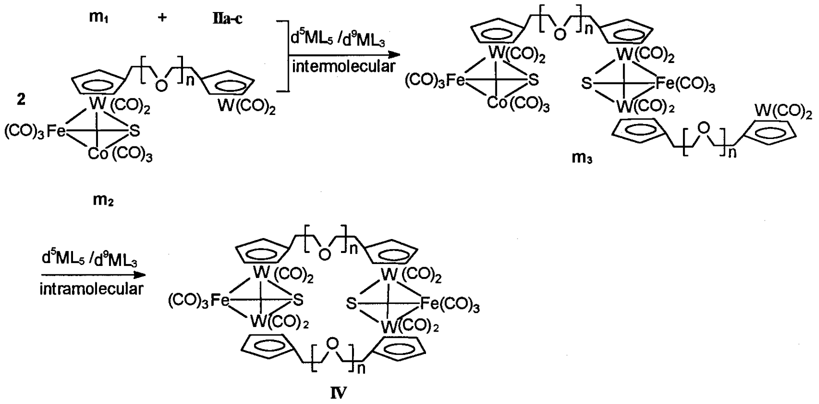

Scheme 5.

Table 5
Electrochemical data for **IIIa–c** [a]

	E (V)	Δ*E* (mV)	I_{pc}/I_{pa}	Cation	$E_{1/2}$ (V)	$\Delta E_{1/2}$ (mV)
IIIa						
	$E_{1/2}+0.56$	82	1.02	no	+0.566	
	$E_{pa1}+0.94$		irr.	Li^+	+0.534	−32
	$E_{pa2}+1.15$		irr.	Na^+	+0.545	−21
	$E_{pc}-1.61$		irr.	K^+	+0.557	−9
IIIb						
	$E_{1/2}+0.60$	88	1.00	no	+0.596	
	$E_{pa1}+1.01$		irr.	Li^+	+0.544	−52
	$E_{pc}-1.53$		irr.	Na^+	+0.583	−13
				K^+	+0.584	−12
IIIc						
	$E_{1/2}+0.55$	83	1.10	no	+0.550	
	$E_{pa1}+0.90$		irr.	Li^+	+0.542	−8
	$E_{pa2}+1.06$		irr.	Na^+	+0.546	−4
	$E_{pa3}+1.31$		irr.	K^+	+0.550	0

[a] Measured in dichloromethane solution containing 0.1 M *n*-Bu_4NPF_6 as supporting electrolyte. Solutions were ca. 1.0×10^{-3} M in crown ether, and potentials were determined with reference to SCE at room temperature (20 ± 1°C) and scan rate 100 mV s^{-1}.

2.4. Cyclic voltammetry of cluster crown ethers *IIIa–c*

Although the electrochemical properties of the simple tetrahedral clusters containing MCoFeE (M = Mo, W; E = S, Se) [27], W_2FeS [28] and $M_2M'_2S_{2-4}$ (M = Mo,W; M′ = Fe Co, Ni) [29] cluster cores were reported some years ago, those of the clusters containing ether structural units have been preliminarily reported just very recently [6]. The electrochemical results, which were obtained from **IIIa–c** in the absence or presence of $LiPF_6$, $NaPF_6$ and KPF_6 are summarized in Table 5. In this table the half-wave potential $E_{1/2}$ is given unless the wave is irreversible (irr.). However, in the latter case an anodic peak potential E_{pa} or a cathodic one E_{pc} is listed. $E_{1/2}$ is identified with the midpoint of E_{pa} and E_{pc} of a cyclic voltammogram, namely, $(E_{pa}+E_{pc})/2$. In addition, the peak potential separation ΔE or $\Delta E_{1/2}$ and peak current ratio I_{pc}/I_{pa} are also given when the wave is reversible or quasi-reversible.

As seen from Table 5, cluster crown ethers **IIIa–c** display three, two, or four oxidation pocesses respectively, when scanning from 0.00 to + 1.50 V versus a standard calomel electrode (SCE). The first oxidation process is reversible, at least quasi-reversible, which has an $E_{1/2}$ value of + 0.55 to + 0.60 V, a I_{pc}/I_{pa} ratio of 1.00 to 1.10 and a redox peak separation ΔE of 82 to 88 mV. The second oxidation process is irreversible with an E_{pa} value of 0.90 to 1.01 V. While the third irreversible oxidation process is observed for **IIIa**,**c** with an E_{pa} value of + 1.15 and + 1.06 V respectively, the fourth irreversible oxidation peak is only observed for **IIIc** with an E_{pa} value of + 1.31 V. However, when scanning from 0.00 to − 1.62 V versus SCE, **IIIc** does not show a reduction wave, whereas **IIIa**,**b** each display an irreversible reduction wave with E_{pc} values of − 1.61 and − 1.53 V, respectively. As mentioned above, cluster crown ethers **IIIa–c** can display one reversible redox process in the range + 0.55 to + 0.60 V. Since this process is easily attainable and could be possibly used in the molecular design of redox-switching devices, we further performed a series of cyclic voltammetry experiments with these crown ethers in the presence of $LiPF_6$, $NaPF_6$ and KPF_6. The electrochemical results are also summarized in Table 5.

As far as a redox-switched system is concerned, complexation with the cation is generally shown to shift the oxidation potential of the redox-active moiety to more positive potential [30–33] and very few were found to shift cathodically [34]. Now, we have found that with the addition of excess amounts of Li^+, Na^+ and K^+ cations as their PF_6^- salts to the electrochemical solutions containing **IIIa–c**, the oxidation potentials of their redox-active cluster cores shift cathodically (except for **IIIc** with KPF_6, no shift). Namely, almost all the potentials $E_{1/2}$ for the cation complexes of the cluster crown ethers shift to lower positive potentials compared with those of the corresponding free crown ether ligands. For example, the half-wave potential of **IIIb** is 52 mV cathodic shift in the presence of $LiPF_6$. This kind of shift can be more clearly seen from the cyclic voltammograms of these cluster crown ethers and their complexes with PF_6^- salts. Fig. 3 shows a comparison of the cyclic voltammogram of **IIIb** with its Li^+ complex. Apparently, such cathodic shifts for these cluster crown ethers in the presence of PF_6^- salts are due to the slight increase in electron density on the cluster cores, in turn making them easier to be oxidized.

3. Experimental

All reactions were carried out under an atmosphere of highly prepurified nitrogen using standard Schlenk or vacuum-line techniques. Tetrahydrofuran (THF) and diglyme were dried and deoxygenated by distillation from sodium-benzophenone ketyl under nitrogen. THF solutions of $Na_2[\eta^5\text{-}C_5H_4CH_2(CH_2OCH_2)_nCH_2C_5H_4\text{-}\eta^5]$ ($n = 1$ [18], $n = 2$, 3 [19]), $[WCoFe(\mu_3\text{-}S)(CO)_8]_2[\eta^5\text{-}C_5H_4CH_2(CH_2OCH_2)_nCH_2C_5H_4\text{-}\eta^5]$ ($n = 1$ [35], $n = 2$, 3 [19]), $[MoCoFe(\mu_3\text{-}S)(CO)_8]_2[\eta^5\text{-}C_5H_4CH_2(CH_2OCH_2)_3\text{-}CH_2C_5H_4\text{-}\eta^5]$ [19] and $FeCo_2(\mu_3\text{-}S)(CO)_9$ [36] were prepared according to literature methods. $W(CO)_6$ and all solvents were available commercially. Dichloromethane used in CV measurements was distilled from CaH_2. $n\text{-}Bu_4NPF_6$ was prepared from $n\text{-}Bu_4NBr$ and HPF_6, whereas $LiPF_6$, $NaPF_6$ and KPF_6 were commercially available and dried by heating in vacuo. Products were separated by preparative TLC (glass plates, 20 × 25 × 0.25 cm; silica gel H, 10–40 μm). IR and ^1H-NMR spectra were recorded on a Nicolet FT-IR 5DX IR spectrophotometer and a Bruker AC-P 200 NMR spectrometer. FAB-MS analysis was carried out on a Zepspec spectrometer. C/H analyses and melting point determination were performed on a Yanaco CHN Corder MT-3 analyzer and a Yanaco MP-500 apparatus, respectively.

3.1. Preparation of $[W_2Fe(\mu_3\text{-}S)(CO)_7]\text{-}[\eta^5\text{-}C_5H_4CH_2CH_2OCH_2CH_2C_5H_4\text{-}\eta^5]$ (**IIIa**)

A 100 ml two-necked flask equipped with a stir-bar, a serum cap and a reflux condenser topped with a N_2 inlet tube, was charged with 0.280 g (0.8 mmol) of $W(CO)_6$, a THF solution of ca. 0.4 mmol of $Na_2(\eta^5\text{-}C_5H_4CH_2CH_2OCH_2CH_2C_5H_4\text{-}\eta^5)$ and 20 ml of diglyme. The mixture was stirred and refluxed for 6 h to give $Na_2[\{W(CO)_3\}_2\{\eta^5\text{-}C_5H_4CH_2CH_2OCH_2CH_2C_5H_4\text{-}\eta^5\}]$ (**Ia**). After removal of solvent, 0.510 g (0.39 mmol) of $[WCoFe(\mu_3\text{-}S)(CO)_8]_2[\eta^5\text{-}C_5H_4CH_2CH_2OCH_2CH_2\text{-}C_5H_4\text{-}\eta^5]$ (**IIa**) and 40 ml of THF were added, and then the mixture was stirred and refluxed for 20 h. After removal of volatiles, the residue was extracted with CH_2Cl_2 and the extracts were subjected to TLC using 2:1 (v/v) CH_2Cl_2–petroleum ether as eluent. From the main brown band was obtained 0.053 g (8%) of **IIIa** as a black solid. m.p. 280°C (dec). Anal. Found: C, 29.62; H, 2.11. Calc. for $C_{21}H_{16}FeO_8SW_2$: C, 29.61; H, 1.89%. IR(KBr disk): terminal C≡O, 2023vs, 1961vs, 1936vs, 1870vs, 1822vs; C–O–C 1127m cm^{-1}. ^1H-NMR (200 MHz, $CDCl_3$): δ 2.85–3.19 (m, 4H, $2C_5H_4CH_2$), 3.62–3.73 (m, 4H, CH_2OCH_2), 5.05, 5.16 (2s, 4H, $2H^2$, $2H^5$), 5.30, 5.43 (2s, 4H, $2H^3$, $2H^4$) ppm. FAB-MS, m/z (^{184}W, rel. intensity): 852 (M^+, 67%), 824 ($M^+ - CO$, 61), 796 ($M^+ - 2CO$, 45), 768 ($M^+ - 3CO$, 100), 740 ($M^+ - 4CO$, 33), 712 ($M^+ - 5CO$, 47), 684 ($M^+ - 6CO$, 44), 654 ($M^+ - 2H\text{–}7CO$, 34).

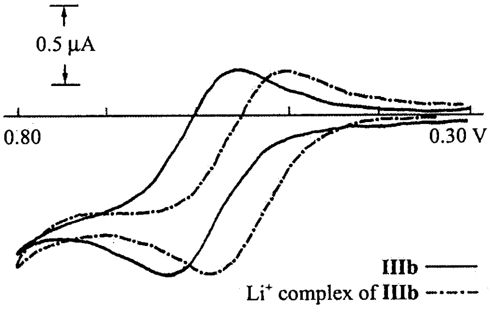

Fig. 3. A comparison between cyclic voltammograms of **IIIb** and its Li^+ complex.

3.2. Preparation of $[W_2Fe(\mu_3\text{-}S)(CO)_7]\text{-}[\eta^5\text{-}C_5H_4CH_2(CH_2OCH_2)_2CH_2C_5H_4\text{-}\eta^5]$ (**IIIb**)

To the same equipped flask described above were added 0.211 g (0.6 mmol) of $W(CO)_6$, a THF solution of ca. 0.3 mmol of $Na_2[\eta^5\text{-}C_5H_4CH_2(CH_2OCH_2)_2\text{-}CH_2C_5H_4\text{-}\eta^5]$ and 10 ml of diglyme. The mixture was stirred and refluxed for 6 h to give $Na_2[\{W(CO)_3\}_2\{\eta^5\text{-}C_5H_4CH_2(CH_2OCH_2)_2CH_2C_5H_4\text{-}\eta^5\}]$ (**Ib**). After removal of solvent, 0.264 g (0.195 mmol) of $[WCoFe\text{-}(\mu_3\text{-}S)(CO)_8]_2[\eta^5\text{-}C_5H_4CH_2(CH_2OCH_2)_2CH_2\ C_5H_4\text{-}\eta^5]$ (**IIb**) and 20 ml of THF were added, and the mixture was stirred and refluxed for 60 h. After removal of volatiles, the residue was extracted with acetone and then the extracts were subjected to TLC using 30:1 (v/v) CH_2Cl_2–Et_2O as eluent. From the main brown band was obtained 0.070 g (20%) of **IIIb** as a black solid. m.p. 240°C (dec). Anal. Found: C, 30.83; H, 2.20. Calc. for $C_{23}H_{20}Fe\ O_9SW_2$: C, 30.83; H, 2.25%. IR (KBr disk): terminal C≡O 2023vs, 1976vs, 1948vs, 1928vs, 1892s, 1866s, 1815s; C–O–C 1124m cm^{-1}. ^1H-NMR (200 MHz, $CDCl_3$): δ 2.75–3.14 (m, 4H, $2C_5H_4CH_2$), 3.64–3.82 (m, 8H, $2(CH_2OCH_2)$), 5.03, 5.16 (2s, 4H, $2H^2$, $2H^5$), 5.32, 5.38 (2s, 4H, $2H^3$, $2H^4$) ppm. FAB-MS, m/z (^{184}W, rel.intensity): 896 (M^+, 66%), 868 ($M^+ - CO$, 18), 840 ($M^+ - 2CO$, 4), 812 ($M^+ - 3CO$, 79), 784 ($M^+ - 4CO$, 9), 756 ($M^+ - 5CO$, 100), 728 ($M^+ - 6CO$, 81), 698 ($M^+ - 2H\text{–}7CO$, 12).

3.3. Preparation of $[W_2Fe(\mu_3\text{-}S)(CO)_7]\text{-}[\eta^5\text{-}C_5H_4CH_2(CH_2OCH_2)_3CH_2C_5H_4\text{-}\eta^5]$ (**IIIc**)

To the flask described above were added 0.176 g (0.5 mmol) of $W(CO)_6$, a THF solution containing ca. 0.25 mmol of $Na_2[\eta^5\text{-}C_5H_4CH_2(CH_2OCH_2)_3CH_2C_5H_4\text{-}\eta^5]$ and 10 ml of diglyme. The mixture was stirred and refluxed for 6 h to give $Na_2[\{W(CO)_3\}_2\{\eta^5\text{-}C_5H_4CH_2\text{-}(CH_2OCH_2)_3CH_2C_5H_4\text{-}\eta^5\}]$ (**Ic**). After removal of solvent, 0.257 g (0.184 mmol) of $[WCoFe(\mu_3\text{-}S)(CO)_8]_2[\eta^5\text{-}C_5H_4CH_2(CH_2OCH_2)_3CH_2\ C_5H_4\text{-}\eta^5]$ (**IIc**) and 25 ml of

Table 6
Crystal data and structural refinements details for **IIIb**,**c**

	IIIb	**IIIc**
Formula	$C_{23}H_{20}FeW_2O_9S$	$C_{25}H_{24}FeW_2O_{10}S$
FW	896.01	940.07
Crystal dimensions (mm)	0.20 × 0.20 × 0.30	0.20 × 0.20 × 0.30
Crystal system	Monoclinic	Monoclinic
Space group	$P2_1/c$ (# 14)	$P2_1$ (# 4)
Unit cell parameters		
a (Å)	14.431(2)	11.369(3)
b (Å)	11.392(3)	17.455(3)
c (Å)	16.260(3)	14.705(6)
β (°)	110.63(1)	109.13(3)
V (Å^3)	2501.5(9)	2756(1)
Z	4	4
D_{calc} (g cm^{-3})	2.379	2.265
F(000)	1680	1776
μ(Mo–K$_\alpha$) (cm^{-1})	98.91	89.83
Temperature (K)	293	293
Wavelength (Å)	0.71069	0.71069
Scan type	ω–2θ	ω–2θ
$2\theta_{max}$ (°)	50	54
No. of observations, n	3446	5348
No. of variables, p	325	609
R	0.026	0.044
Rw	0.033	0.052
Goodness-of-fit	1.27	1.81
Largest difference peak (e Å^{-3})	0.73	2.39

THF were added,and the mixture was stirred and refluxed for 60 h. After removal of volatiles, the residue was extracted with acetone and the extracts were subjected to TLC using 3:2 (v/v) THF–petroleum ether as eluent. From the main brown band was obtained 0.100 g (29%) of **IIIc** as a black solid. m.p. 200°C (dec). Anal. Found: C, 31.77; H, 2.52. Calc. for $C_{25}H_{24}Fe\ O_{10}SW_2$: C, 31.94; H, 2.57%. IR (KBr disk): terminal C≡O 2026vs, 1965vs, 1922vs, 1906s,1892s, 1854s, 1833vs; C–O–C 1108m cm^{-1}. ^{1}H-NMR (200 MHz, $CDCl_3$): δ 2.63–2.98 (m, 4H, $2C_5H_4CH_2$), 3.47–3.79 (m, 12H, $3(CH_2OCH_2)$), 5.10, 5.14 (2s, 4H, 2H^2, 2H^5), 5.34, 5.69 (2s, 4H, 2H^3, 2H^4) ppm. FAB-MS, m/z (^{184}W, rel. intensity): 940 (M$^+$, 37%), 856 (M$^+$ − 4H−3CO, 100), 800 (M$^+$ − 5CO, 85), 772 (M$^+$ − 6CO, 27).

*3.4. Preparation of [$W_2Fe(\mu_3$-S)(CO)$_7$][η^5-$C_5H_4CH_2(CH_2OCH_2)_3CH_2C_5H_4$-$\eta^5$] (**IIIc**) and [$Mo_2Fe(\mu_3$-S)(CO)$_7$][$\eta^5$-$C_5H_4CH_2(CH_2OCH_2)_3CH_2C_5H_4$-$\eta^5$] (**IV**)*

To the flask described above were added 0.352 g (1.0 mmol) of $W(CO)_6$, a THF solution containing ca. 0.5 mmol of $Na_2[\eta^5$-$C_5H_4CH_2(CH_2OCH_2)_3CH_2C_5H_4$-$\eta^5]$ and 20 ml of diglyme. The mixture was stirred and refluxed for 6 h to give $Na_2[\{W(CO)_3\}_2\{\eta^5$-$C_5H_4CH_2(CH_2OCH_2)_3CH_2C_5H_4$-$\eta^5\}]$ (**Ic**). After removal of the solvent, 0.490 g (0.4 mmol) of [MoCoFe(μ_3-S)(CO)$_8$]$_2$[η^5-$C_5H_4CH_2(CH_2OCH_2)_3$ $CH_2C_5H_4$-η^5] and 30 ml of THF were added, and then the mixture was stirred and refluxed for 60 h. After removal of volatiles, the residue was extracted with acetone and then the extracts were subjected to TLC using 3:2 (v/v) THF–petroleum ether as eluent. From the first main band was obtained a mixture, which was further subjected to TLC separation using CH_2Cl_2 as eluent. From the first brown band was obtained 0.096 g (31%) of **IV** as a black solid. From the second brown band was obtained 0.055 g (12%) of **IIIc** as a black solid. **IIIc** and **IV** [6] have been identified by their melting point, IR and ^{1}H-NMR spectroscopies.

*3.5. X-ray structure determinations of **IIIb**,**c***

Single-crystals of **IIIb and IIIc** suitable for X-ray diffraction analyses were grown by slow evaporation of their CH_2Cl_2–hexane solutions at about 4°C. Each crystal was mounted on a Rigaku AFC7R diffractometer with a graphite monochromator with Mo–K$_\alpha$ radiation (λ = 0.71069 Å). Details of the crystal data, data collections and structure refinements are summarized in Table 6. The structures were solved by direct methods and expanded by Fourier techniques. The final refinements were accomplished by the full-matrix least-squares method with anisotropic thermal parameters for non-hydrogen atoms. The calculations for **IIIa**–**c** were performed using the TEXSAN crystallographic software package of the Molecular Structure Corporation.

*3.6. Cyclic voltammetry measurements of **IIIa**–**c***

Cyclic voltammetry measurements were performed using a BAS-100B electrochemical analyzer and were carried out in dichloromethane solution containing 0.1 M n-Bu_4NPF_6 using a platinum working electrode (φ = 1 mm) and a platinum wire counter electrode, with ferrocene, $E_{1/2}$ = 0.41–0.42 V, as internal reference. All potential values are quoted relative to SCE.

The dichloromethane solution, ca. 1.0×10^{-3} M in cluster compound or ca. 5.0×10^{-3} M in $LiPF_6$, $NaPF_6$ or KPF_6, was placed in a single-compartment electrochemical cell and degassed by bubbling with argon for 5 min before measurement. An argon atmosphere was continuously maintained above the solution while the experiments were in progress. The platinum working electrode surface was polished with 0.05 μm alumina, sonicated in distilled water, and air dried immediately before use.

4. Supplementary material

Crystallographic data for the structures reported in this paper have been deposited with the Cambridge

Crystallographic Data Centre, CCDC nos. 145088 for **IIIb** and 145239 for **IIIc**. Copies of this information may be obtained free of charge from The Director, CCDC, 12 Union Road, Cambridge, CB2 1EZ, UK (Fax: +44-1223-336033; e-mail: deposit@ccdc.cam.ac.uk or www: http://www.ccdc.cam.ac.uk).

Acknowledgements

We are grateful to the National Natural Sience Fundation of China, Laboratory of Organometallic Chemistry and State Key Laboratory of Structural Chemistry for financial support of this work.

References

[1] G.W. Gokel, Crown Ethers and Cryptands, Monographs in Supramolecular Chemistry, Royal Society of Chemistry, Cambridge, 1991.
[2] B. Dietrich, P. Viout, J.-M. Lehn, Macrocyclic Chemistry, VCH, Weinheim, 1993.
[3] F. Vögtle, Supramolecular Chemistry, An Introduction, Wiley, Chichester, 1991.
[4] J.-M. Lehn, Supramolecular Chemistry, Concepts and Perspectives, VCH, Weinheim, 1995.
[5] F.C.J.M. van Veggel, W. Verboom, D.N. Reinhoudt, Chem. Rev. 94 (1994) 279.
[6] L.-C. Song, D.-S. Guo, Q.-M. Hu, X.-Y. Huang, Organometallics 19 (2000) 960.
[7] (a) N.D. Lowe, C.D. Garner, J. Chem. Soc. Dalton Trans. (1993) 2197. (b) N.D. Lowe, C.D. Garner, J. Chem. Soc. Dalton Trans. (1993) 3333.
[8] E. Solari, W. Lesueur, A. Klose, K. Schenk, C. Floriani, A. Chiesi-Villa, C. Rizzoli, J. Chem. Soc. Chem. Commun. (1996) 807.
[9] M. Moran, C.M. Casado, I. Cuadrado, J. Losada, Inorg. Chim. Acta 185 (1991) 33.
[10] E. Fu, J. Granell, M.L.H. Green, V.J. Lowe, S.R. Marder, G.C. Saunders, M. Tuddenham, J. Organomet. Chem. 355 (1988) 205.
[11] H. Plenio, R. Diodone, J. Org. Chem. 58 (1993) 6650.
[12] H. Plenio, D. Burth, Organometallics 15 (1996) 1151.
[13] S. Bélanger, M. Gilbertson, D.I. Yoon, C.L. Stern, X. Dang, J.T. Hupp, J. Chem. Soc. Dalton Trans. (1999) 3407.
[14] (a) T. Izumi, T. Tezuka, S. Yusa, A. Kasahara, Bull. Chem. Soc. Jpn. 57 (1984) 2435. (b) M.C. Grossel, M.R. Goldspink, J.A. Hriljac, S.C. Weston, Organometallics 10 (1991) 851. (c) H. Plenio, C. Aberle, Angew. Chem. Int. Ed. Engl. 37 (1998) 1397. (d) G.C. Dol, P.C.J. Kamer, F. Hartl, P.W.N.M. van Leeuwen, R.J.M. Nolte, J. Chem. Soc. Dalton Trans. (1998) 2083. (e) J.C. Medina, T.T. Goodnow, M.T. Rojas, J.L. Atwood, B.C. Lynn, A.E. Kaifer, G.W. Gokel, J. Am. Chem. Soc. 114 (1992) 10583.
[15] (a) P.D. Beer, A.D. Keefe, H. Sikanyika, C. Blackburn, J.F. McAleer, J. Chem. Soc. Dalton Trans. (1990) 3289. (b) T. Izumi, S. Murakami, A. Kasahara, Bull. Chem. Soc. Jpn. 61 (1988) 3565.
[16] (a) P.D. Beer, Acc. Chem. Res. 31 (1998) 71. (b) P.D. Beer, A.D. Keefe, J. Organomet. Chem. 375 (1989) C40.
[17] (a) J.R. Farrell, C.A. Mirkin, L.M. Liable-Sands, A.L. Rheingold, J. Am. Chem. Soc. 120 (1998) 11834. (b) J.R. Farrell, C.A. Mirkin, I.A. Guzei, L.M. Liable-Sands, A.L. Rheingold, Angew. Chem. Int. Ed. Engl. 37 (1998) 465.
[18] L.-C. Song, Y.-B. Dong, Q.-M. Hu, J. Sun, Organometallics 15 (1996) 1954.
[19] L.-C. Song, D.-S. Guo, Q.-M. Hu, J. Chem. Res. (S) (1999) 516.
[20] J.P. Collman, L.S. Hegedus, J.R. Norton, R.G. Finke, Principles and Applications of Organotransition Metal Chemistry, University Science Books, Mill Valley, CA, 2nd Edn., 1987.
[21] D.M. Curtis, K.R. Han, W.M. Butler, Inorg. Chem. 19 (1980) 2096.
[22] J.R. Dyer, Applications of Absorption Spectroscopy of Organic Compounds, Prentice-Hall, Englewood Cliffs, NJ, 1965.
[23] L.-C. Song, J.-Y. Shen, Q.-M. Hu, R.-J. Wang, H.-G. Wang, Organometallics 12 (1993) 408.
[24] R. Hoffmann, Angew. Chem. Int. Ed. Engl. 21 (1982) 711.
[25] H. Vahrenkamp, Comments Inorg. Chem. 4 (1985) 253.
[26] (a) L.-C. Song, J.-Y. Shen, Q.-M. Hu, X.-Y. Huang, Organometallics 14 (1995) 98. (b) L.-C. Song, Y.-B. Dong, Q.-M. Hu, X.-Y. Huang, J. Sun, Organometallics 16 (1997) 4540. (c) L.-C. Song, J.-Y. Shen, Q.-M. Hu, B.-S. Han, R.-J. Wang, H.-G. Wang, Inorg. Chim. Acta 219 (1994) 93. (d) L.-C. Song, Y.-B. Dong, Q.-M. Hu, Y.-K. Li, J. Sun, Polyhedron 17 (1998) 1579. (e) L.-C. Song, Y.-K. Li, Q.-M. Hu, J. Sun, J. Coord. Chem. 45 (1998) 1.
[27] U. Honrath, H. Vahrenkamp, Z. Naturforsch. Teil B 39 (1984) 545.
[28] P.D. Williams, M.D. Curtis, J. Organomet. Chem. 352 (1988) 169.
[29] M.D. Curtis, P.D. Williams, W.M. Butler, Inorg. Chem. 27 (1988) 2853.
[30] P.D. Beer, Chem. Soc. Rev. 18 (1989) 409.
[31] C.D. Hall, N.W. Sharpe, I.P. Danks, Y.P. Sang, J. Chem. Soc. Chem. Commun. (1989) 419.
[32] C.D. Hall, S.Y.F. Chu, J. Organomet. Chem. 498 (1995) 221.
[33] H. Plenio, C. Aberle, Chem. Commun. (1998) 2697.
[34] C.D. Hall, N. Sachsinger, S.C. Nyburg, J.W. Steed, J. Organomet. Chem. 561 (1998) 209.
[35] L.-C. Song, D.-S. Guo, Y.-B. Dong, Transition Met. Chem. 25 (2000) 37.
[36] M. Cowie, R.L. DeKock, T.R. Wagenmaker, D. Seyferth, R.S. Henderson, M.K. Gallagher, Organometallics 8 (1989) 119.